Running Title: Rapid Kinetic Techniques

RAPID KINETIC TECHNIQUES

John F. Eccleston[1*], Stephen R. Martin[1], and Maria J. Schilstra[2]

[1)] Division of Physical Biochemistry

National Institute for Medical research

The Ridgeway, Mill Hill, London NW7 1AA, U.K.

[2)] Biological and Neural Computation Group

Science & Technology Research Institute

University of Hertfordshire, College Lane

Hatfield AL10 9AB, U.K.

(*) To whom correspondence should be addressed.

e-mail: jeccles@nimr.mrc.ac.uk

I. Abstract

The elementary steps in complex biochemical reaction schemes (isomerization, dissociation, and association reactions) ultimately determine how fast any system can react in responding to incoming signals, and in adapting to new conditions. Many of these steps have associated rate constants that result in sub-second responses to incoming signals, or externally applied changes. This chapter is concerned with the techniques that have been developed to study such rapidly reacting systems *in vitro*, and to determine the values of the rate constants for the individual steps. We focus principally on two classes of techniques: 1) flow techniques, in which two solutions are mixed within a few milliseconds, and the ensuing reaction monitored over milliseconds to seconds, and 2) relaxation techniques, in which a small perturbation to an existing equilibrium is applied within a few microseconds, and the response of the system is followed over microseconds to hundred of milliseconds. These reactions are most conveniently monitored by recording the change in some optical signal, such as absorbance or fluorescence. We discuss the instrumentation that is (commercially) available to study fast reactions, and describe a number of optical probes (chromophores) that can be used to monitor the changes. We discuss experimental design appropriate for the different experimental techniques and reaction mechanisms, as well as the fundamental theoretical concepts behind the analysis of the data obtained.

II. Introduction

A large number of important biological processes must obviously occur on timescales of very much less than a second. By way of illustration, consider the position of a cricket batsman (or baseball batter); for very fast deliveries as little as 400 milliseconds may elapse between the ball leaving the bowler's (pitcher's) hand and it reaching the batter's bat. During this short time, a whole series of processes occur in the batter's eyes, brain, nerves and muscles, which all involve the interaction of a wide variety of different molecules. The first steps towards understanding what happens in these processes include identification of the participants, and sketching out reaction pathways and interaction networks. The next step consists of a thorough characterization of the dynamics of the interactions. This information is essential if one wishes to create a quantitative picture of such processes, evaluate the 'dynamic range' of their constituents, assess the conditions under which systems will function optimally, and, most importantly, predict under which conditions they will fail.

The majority of biochemical reactions are reversible, and, when studied in isolation in the 'test tube', will reach an equilibrium state, with reactant and product concentrations determined by the equilibrium constant, *K*. Once this equilibrium state has been reached, the concentrations of the individual species involved will remain constant, unless the system is perturbed in some way. Reaction systems may be perturbed by the influx or efflux of reactants, but also by changes in some external parameter, such as temperature. A change in temperature induces a perturbation because equilibrium constants are generally dependent on temperature ($K = e^{-\Delta G/RT}$, and $\Delta G = \Delta H - T\Delta S$, where ΔG, ΔH, and ΔS are the changes in free energy, enthalpy, and entropy, respectively, R is the universal gas constant, and T is the absolute temperature).

The speed at which any individual reaction or reaction network can respond following such a perturbation depends on the rates of the different elementary steps. Generally speaking, the more dynamic a system, that is, the larger its forward *and* reverse reactions, the more quickly it will reach the new equilibrium position. Although the cell is, of course, a non-equilibrium system, it is important to remember that any reaction network that can reach equilibrium rapidly will also be able to rapidly reach other 'target' states. Thus, it is the rates of the elementary steps that ultimately determine how fast a system can react, respond to incoming signals, and adapt to new conditions. In any biochemical reaction these elementary steps are either unimolecular (an isomerization of a single entity, or the dissociation of a complex) or bimolecular processes (association of two molecules or complexes) that occur almost exclusively on sub-second, often sub-millisecond, time scales. To study these reactions, instrumentation is required that allows the investigator 1) to rapidly mix the reactants or perturb the system in a controlled way, and 2) to monitor the concentrations of one or more reaction partners with sufficient time resolution as the reaction proceeds.

There are various ways of monitoring the concentration of participants during a reaction. For example, samples may be taken from the reaction volume, mixed with a chemical quenching

agent to stop the reaction, and their contents assessed by chromatography, electrophoresis, or mass spectrometric techniques. Such methods can directly determine the concentrations of different reaction participants in a relatively straightforward way, but they are discontinuous and have a limited time resolution that depends on the sampling rate that can be achieved. A more common approach is to take advantage of changes in optical signals, such as absorbance, circular dichroism, or fluorescence, which often accompany a reaction. Although spectroscopic methods do not generally permit the direct determination of concentrations of individual species, they are continuous and can achieve high precision and time resolution. Unfortunately, most conventional spectrophotometers cannot be used to study reactions that are complete within less than about 10 seconds, as it takes at least that amount of time to mix the reagents, close the sample compartment, and activate the instrument, or to increase the temperature of the reaction mixture. This chapter is therefore concerned with the application of techniques that have been developed to overcome these problems. We will focus on the two principal classes of methods:

a. *Flow* (or *rapid mixing*) techniques, which are essentially an extension of the classical 'mix and observe' approach, and

b. *Relaxation* techniques, in which a system at equilibrium is perturbed by applying a rapid change in an external parameter, such as temperature or pressure.

Methods such as X-ray crystallography, NMR, and equilibrium binding studies, which yield the necessary (static) structural and thermodynamic information, are complemented by flow and relaxation methods, which yield the kinetic information that is indispensable for understanding the dynamics of biochemical processes.

III. Basic theory

In the following, we shall use the symbols P and L to indicate the participants in simple first- and second-order processes (reaction steps whose kinetics are determined by the concentration of one or two reactants, respectively). P and L stand for "protein" and "ligand" – as many intracellular interactions are between proteins and smaller molecules – but may represent any two reactants, proteins, DNA, lipids, biomolecular assemblies, etc. PL denotes a complex between P and L, and P*, L* and PL* indicate different conformational states of P, L, and PL.

A. First-order reactions

The simplest reversible reaction is one where the forward and reverse steps are both unimolecular processes with first-order rate constants k_{+1} and k_{-1} (units s^{-1}) for the forward and reverse steps.

[SCHEME **I** HERE]

The equilibrium constant, K, for this reaction is defined as $K = k_{+1}/k_{-1}$, which is dimensionless. There is no net influx or efflux of material, so that $[P] + [P^*] = P_{tot}$, where square brackets indicate instantaneous (or current) concentrations, and P_{tot} is the total concentration of protein. The rate $d[P^*]/dt$ at which P* is formed is given by:

$$\frac{d[P^*]}{dt} = k_{+1}[P] - k_{-1}[P^*] = k_{+1}P_{tot} - (k_{+1} + k_{-1})[P^*] \quad (1)$$

Note that this rate may be positive (P* is being formed) as well as negative (P* is disappearing). Equation 1 has an analytical solution that expresses the concentration of P* as a function of time:

$$[P^*](t) = P^*_{eq} + \left(P^*_0 - P^*_{eq}\right) \cdot e^{-k_{OBS}\,t} \quad (2)$$

Here k_{OBS}, which is equal to $k_{-1} + k_{+1}$, is called the *observed rate* of the reaction. P^*_0 and P_{eq} are the initial and equilibrium (or final) concentrations of P* (see below). Figure **1** shows the change in $[P^*]$ with time for several different combinations of P^*_0 and k_{OBS}. These curves are known as transients, and illustrate the following concepts.

a. **Equilibrium.** If P^*_0 is not equal to P^*_{eq} (for example if the system is subjected to a sudden change in pH, which alters the equilibrium constant), the concentrations of P and P* will change, until the altered equilibrium position is reached, and the concentrations of P and P* are constant. P^*_{eq}, the equilibrium concentration of P*, is equal to $(P_{tot}K)/(1+K)$, which is equal to $k_{+1}P_{tot}/k_{OBS}$.

b. **Amplitude.** The difference between the concentration of P* at the beginning and the end of the reaction (at equilibrium), $P^*_{eq} - P^*_0$, is called the reaction *amplitude*, $\Delta[P^*]$.

c. **Observed rate.** Equation 2 is a single exponential function, whose shape and amplitude is fully defined by k_{OBS}, P^*_{eq}, and P^*_0. The larger k_{OBS}, the more rapidly the system will reach equilibrium. Because k_{OBS} is equal to the sum of the individual rate constants, two reversible reactions with the same k_{+1} but different k_{-1} values will reach equilibrium at different rates, and the one with the *largest* k_{-1} will equilibrate fastest (Compare curves D and E in Figure **1**c).

d. **Rate constants from observed rates.** Analysis of the change of $[P^*]$ with time will yield k_{OBS}, not the individual rate constants. However, when the equilibrium constant K is known, the individual rate constants can be calculated as follows:

$$k_{-1} = \frac{k_{OBS}}{1+K}, \quad k_{+1} = \frac{K \cdot k_{OBS}}{1+K} \quad \textbf{(3)}$$

e. **Relaxation time and half life.** The reciprocal of k_{OBS} is called the *relaxation time*, or *time constant*, τ, of the system. At $t = \tau$, the difference between $[P^*]$ and $[P^*_{eq}]$ will have decreased to $1/e$ of the total amplitude $\Delta[P^*]$, *independent* of the value of P^*_0.

The *half life* $t_{1/2}$ of the reaction is defined as the time taken for the difference between [*P**] and [P^*_{eq}] to decrease to half of the total amplitude, and relates to the relaxation time and observed rate as $t_{1/2} = 0.693\tau = 0.693/k_{OBS}$ (ln(0.5) = -0.693). It should be emphasized that although k_{OBS} and τ^{-1} are identical, the former is generally used to describe transients observed in flow experiments, whereas the latter is generally used to describe relaxation (or small perturbation) experiments.

B. Second-order reactions

Reversible binding reactions, such as those in which a ligand associates with a protein, include a second-order association process, and a first-order dissociation, and are described by:

[SCHEME **II** HERE]

Here k_{+1} is the second-order association rate constant (units: $M^{-1}s^{-1}$) and k_{-1} is the first-order dissociation rate constant (units: s^{-1}). The *equilibrium dissociation constant* for this reaction, K_d, is equal to k_{-1}/k_{+1} (units: M), whereas the *equilibrium association constant*, K_a, is its reciprocal (k_+/k_-, units: M^{-1}). There are now two conservation equations that must be obeyed: [*P*] + [*PL*] = P_{tot} and [*L*] + [*PL*] = L_{tot}, where P_{tot} and L_{tot} are the total concentrations of P and L. The rate *d*[*PL*]/*dt* at which PL is formed is given by:

$$\frac{d[PL]}{dt} = k_{+1}[P][L] - k_{-1}[PL] = k_{+1}(P_{tot} - [PL])(L_{tot} - [PL]) - k_{-1}[PL] \qquad (4)$$

This equation does not have a simple analytical solution (a general bimolecular equivalent of equation 2) that describes the change in [PL] as a function of time for given initial and total concentrations of P, L, and PL. However, under certain special conditions, the solution to equation 4 can be shown to be very similar to equation 2.

1. Pseudo-first-order conditions

If one of the reactants is in large excess over the other (L_{tot} » P_{tot} or L_{tot} » P_{tot}), the concentration of the component in excess remains effectively constant during the whole time course, because $X_{tot} - [PL] \approx X_{tot}$, where X_{tot} is the concentration of the component present in excess. Equation 4 then simplifies to equation 1, with $k_{+1}X_{tot}$ instead of k_{+1}. As a result, the formation of PL is said to follow pseudo first-order kinetics, with an observed rate k_{OBS} given by:

$$k_{OBS} = t^{-1} = k_{+1}X_{tot} + k_{-1} \qquad (5)$$

Such conditions are generally employed in flow experiments.

2. Near equilibrium conditions

It can be shown that the change in concentration of PL also approaches first-order kinetics when the concentrations of P and L are very close to their equilibrium values (Caldin, 1964). This is because the changes in the concentrations of all species are then very small compared to the values of the concentrations themselves, and therefore may be regarded as being constant. Such conditions can be introduced by a small perturbation of the system, for example by increasing the temperature or pressure of the reaction volume by a small amount (see Section IV.B), thereby slightly changing the equilibrium constant for the system. Before the change, P and L are at their equilibrium concentrations under the current conditions. If the change is applied virtually instantaneously, the concentrations will still be at their old values immediately after the jump. At that point, the system is out of equilibrium, but will immediately begin to relax toward the new equilibrium, where [P] and [L] are slightly different. In this case, the expression for the reciprocal relaxation time is:

$$t^{-1} = k_{+1}([P] + [L]) + k_{-1} \tag{6}$$

IV. Techniques

In this section we introduce the two major groups of techniques used in the study of rapid reactions: flow and relaxation techniques. These techniques differ in their time scales of applicability: flow methods are generally used to study reactions that occur on timescales varying from a few milliseconds to tens of seconds, whereas relaxation techniques are applicable to reactions that happen within microseconds to hundreds of milliseconds.

A. Flow techniques

All flow techniques use special mixing chambers that are designed to mix two solutions containing the appropriate reactants. The solutions are generally driven at high velocity into the mixing chamber in order to achieve mixing that is both rapid and complete. Reactions cannot, in general, be monitored inside the mixing chamber itself, so that the mixed solution can only be observed at some point 'downstream' from the mixing chamber. Because the mixing and subsequent flow to the point of observation take a finite amount of time, the mixed solution already has a certain average 'age'[1] before it can be observed. The time during which the reaction cannot be monitored is called the *dead time* of the instrument.

1. Stopped-flow

Of all the rapid reaction techniques, stopped-flow comes closest to being a standard laboratory technique. As with all flow techniques, the two reactant solutions are rapidly mixed by driving them from 'drive' syringes into an appropriately designed mixing chamber.

[1] Because mixing is not instantaneous, there will be a certain spread in the age of the mixed solution. An effective mixing chamber produces a mixed solution in which the spread is relatively small.

Following mixing, the solution flows into an observation chamber, and the flow is stopped using a 'stopping' syringe (Eccleston et al., 2001). The reaction is then followed by monitoring the change in some suitable optical signal, generally absorption or fluorescence, as a function of time. The effective dead time of the instrument is determined by the time it takes to start and stop the flow, and is typically 1 to 2 ms. Reactions with half times shorter than this dead time cannot be studied. Reactions with very long half times (> 10 s) can, at least in principle, be studied using the stopped-flow technique. In practice, the study of very slow reactions may be complicated by lamp instabilities and, in the case of fluorescence, by photobleaching of the chromophore. The latter effect can generally be reduced by the use of an automatic shutter so that the reaction mixture is not constantly illuminated by light.

Commercial equipment is available from several sources (see section V). These devices range from stand-alone models with a variety of detection modes to small, hand-driven devices that can be used in conjunction with regular spectrophotometers. The latter are relatively inexpensive and permit the study of reactions with half times as short as 10 ms (although this also depends on the response time of the spectrometer) and are useful for studying many reactions. Most stopped-flow instruments are designed to mix equal volumes of the two reactants, but some will allow different volumes to be used. This particular technique is most widely used in studies of protein folding using chemical denaturants, where large and rapid changes in the concentration of denaturant are required. Devices that permit double mixing experiments are also available: two reactants are mixed and this mixed solution is then rapidly mixed with a third solution after a variable pre-selected time. This approach allows the study of the reactions of short-lived intermediates and has been used to provide important information in the study of several enzyme mechanisms.

2. Quenched flow

In the quenched flow method the two reactant solutions are rapidly mixed as in the stopped flow method and then flow down an 'aging tube' at constant velocity before being mixed with a 'quenching agent', which stops the reaction. The age of the quenched sample is determined by the flow rate and volume of the flow tube, so by doing a series of experiments with different flow rates and flow tube volumes a series of time points can be built up. The most frequently used quenching agent is acid, but alternative quenchers, such as metal chelators (EDTA or EGTA), can be used in the case of some metal-dependent reactions. The quenched reaction mixture is collected and analyzed using an appropriate method, such as HPLC, to separate reactant and product. Time points between ~5 ms and ~150 ms can usually be obtained in this way. In principle, points at longer times could be obtained by using longer flow tubes and/or slower flow rates. However, in the former case excessively large amounts of material would be used and in the latter case, the flow would not be fast enough to obtain the turbulent flow necessary for rapid and efficient mixing. An alternative approach is to operate the instrument in the 'pulsed flow' mode where the mixed solution passes down the flow tube but before reaching the quenching solution flow is stopped for an electronically controlled time

before being resumed. In this case, the age of the quenched sample is a combination of flow rate, flow tube volume, and the delay time, although the first two become negligible at times of longer than a few seconds. Although quenched flow methods are much more labor intensive than stopped-flow methods, they do have the advantage that they can be used when no optical signal is available. In addition, it is one of the few experimental techniques that can be used to give unequivocal information about steps involving the formation or cleavage of covalent bonds.

3. Continuous flow

In this method the two reactants are pumped at high velocity into a small volume mixing chamber. The optical signal is monitored at different points downstream from the mixer in the direction of the flow and translated into the time-dependent signal change on the basis of the known flow rate. Historically, stopped-flow was first developed from the earlier continuous flow method, and has almost completely been preferred to continuous flow because of its better sample economy and the ability to measure the kinetics out to long times. However, continuous flow can measure reactions on a much faster time scale than stopped-flow and Shastry et al. (1998) have recently shown that the efficiency of the method can be greatly improved by using a CCD camera to image the flow tube and the distance down the flow tube is converted to time from the linear flow rate. By combining this improved detection method with a very efficient capillary mixer, they were able to achieve mixing times of ~15 μs and dead times as short as 45 μs.

B. Relaxation techniques

Reactions that are too fast to be studied using rapid mixing techniques can be studied using techniques in which a system at equilibrium is perturbed by applying a rapid change in some external parameter. In each of the techniques discussed below, the response of the system to the new conditions is then monitored by recording a suitable optical signal.

1. Temperature jump

The best known relaxation technique is the temperature-jump method, which has been available for several decades. In this technique, the perturbation consists of a sudden increase in the temperature of the solution. In the most common setup, the temperature jump is brought about by Joule heating, the temperature increase in a conducting solution resulting from the resistance to an electric current flowing through it. Discharge of a high voltage capacitor through the solution is used to produce temperature jumps of up to 5 $^{\circ}$C in as little as 1 to 2μs. Therefore, reactions with half times shorter than this temperature rise time cannot be studied using Joule heating devices. However, laser heating devices can be used to produce large increases in temperature in relatively small irradiated volumes in much shorter times, as little as 10 ns (see e.g. Turner et al., 1972, Williams et al., 1996).

In Joule heating devices the solution will begin to cool immediately after the jump, owing to equilibration with the cell body, optical windows, electrodes, etc. The temperature of the heated volume decays to ambient temperature with a half-life of the order of 50 s depending on the precise geometry of the device. Therefore, reactions with half times longer than several hundred milliseconds are difficult to study. However, in some cases applying the cooling corrections described by (Rabl, 1979) can extend this upper limit. In laser heating devices the small heated volume decays to ambient temperatures with a much shorter half-life.

2. Pressure jump

In the pressure jump method, which has also been available for several decades, the equilibrium is perturbed by applying a rapid change in pressure rather than temperature. Recent technical advances (see, for example, Pearson et al., 2002) have led to the development of devices that use piezoelectric crystals to generate large pressure increases (of up to 200 atmospheres) in small samples (~50 µl) in as little as 50 µsec. Although pressure induced perturbations are very much smaller than those produced by temperature changes, high repetition rates can be used (because there is no equivalent of a cooling phase in a pressure-jump experiment) and this allows the collection of data with very good signal to noise ratio. In addition, the pressure jump technique has several distinct advantages over the temperature jump method: 1) reactions can be followed on long time scales when required because the pressure remains constant after the jump, 2) samples do not require the high ionic strength needed for efficient Joule heating in temperature jump devices, and 3) jumps can be recorded in both directions. In addition, intrinsic fluorescence signals (such as those from tryptophan in proteins) show little pressure sensitivity over the range used for perturbation kinetics, so there is no transient associated with the jump itself, in contrast to the effect of a temperature change.

C. Flash photolysis

Flash photolysis, in which a reaction is triggered by a pulse of light, was previously limited to the study of intrinsically light-dependent reaction systems, such as those involved in visual processes. In recent years the applicability of the technique has been significantly extended by the development of methods in which a ligand for a particular reaction is converted to an inactive form by the addition of a caging group that can be converted by light into the natural, active form. Caged compounds release the active ligand species, generally on a millisecond or faster time scale, upon flash photolysis with near-UV light. They are used principally in studies of rapid biological processes to enable the application of a particular ligand at or near its site of action. Many caged compounds have now been developed, ranging from caged nucleotides such as ATP to caged forms of neuroexcitatory amino acids such as L-glutamate. It is also possible to produce a pH jump by flashing an aqueous solution containing a suitable

photolabile caged compound, such as *o*-nitrobenzaldehyde, with a nanosecond UV laser (see, for instance, Gutman and Nachliel, 1990, Abbruzzetti et al., 2000).

A somewhat different philosophy was used in the development of the widely used caged calcium compounds. The three commercially available caged calcium compounds (DM-nitrophen, nitrophenyl-EGTA, and nitr-5) bind calcium with very high affinity (K_d 5 - 150 nM) but can be rapidly photolysed into photoproducts with very much lower affinity for calcium (K_d 0.01 to 1 mM). Locally applied flashes of light release calcium from the cage, and thus produce rapid and large increases in calcium concentration.

Further detailed discussion of these particular techniques is beyond the scope of this chapter. However, the analysis of the results obtained using such approaches is based on the same general principles as those outlined in subsequent sections.

V. Instrumentation

Instruments for the study of fast reactions are commercially available from a number of different suppliers: TgK Scientific Ltd (Supplier of HiTech instruments: http://www.hi-techsci.com/); KinTek Corporation (http://www.kintek-corp.com/); OLIS (http://olisweb.com/); Applied Photophysics (http://www.photophysics.com/); and Biologic Science Instruments (http://www.bio-logic.info/). The principal optical detection modes employed are fluorescence and absorbance. Fluorescence detection is now very widely employed because it is intrinsically much more sensitive than absorption and therefore permits measurements to be made at very low concentrations in many cases. Although circular dichroism (CD) detection is widely employed in studies of protein unfolding the inherently poor signal to noise ratios of CD signals limits its use in the study of protein-ligand interactions. Florescence measurements will therefore be the main focus of this section.

A. Instrument characteristics

As with any scientific instrument it is important that user understand the characteristics and limitations of the equipment being used.

In the case of stopped-flow, for example, it is important 1) to demonstrate that mixing is efficient, and 2) to determine the dead time of the instrument. Mixing efficiency can be tested by rapidly mixing a solution of a pH indicator above its pK_a with buffer at a pH below its pK_a. For example, a 1 µM solution of 4-methylumbelliferone in 0.1 M sodium pyrophosphate, pH 8.7, is initially mixed with 0.1 M sodium pyrophosphate, pH 8.7 alone and the signal observed. The syringe containing buffer alone in then replaced by 0.1 M sodium pyrophosphate, pH 6.2, and then mixed with the 4-methylumbelliferone. Because proton transfer reactions are effectively instantaneous on the time scale of a stopped-flow experiment the *absence* of any detectable reaction is taken to indicate that mixing is efficient. The instrumental dead time can be measured using any well-characterized second-order reaction that has a large change in an appropriate optical signal. The reaction of N-acetyl tryptophanamide (NATA) with N-

bromosuccinimide in 0.1 M sodium phosphate, pH 7.5 can be used for fluorescence measurements. The true starting signal for the reaction is determined by mixing 10 uM NATA in 0.1 M sodium phosphate, pH 7.5 with buffer alone. With excitation at 280 nm, emission is observed through a 320 nm cut-off filter and a suitable signal obtained. Then the NATA solution is mixed with 600 µM N-bromosuccinimide. The reaction is therefore performed under pseudo first-order conditions with concentrations chosen to give a known half time of the order of 20 ms (see section VII). Extrapolation of the observed signal back to the true starting signal using the known half time gives the dead time. Detailed protocols for performing dead time measurements and for the investigation of mixing efficiency are given by (Eccleston, et al., 2001).

In order to do a temporal calibration of a quenched-flow instrument, the alkaline hydrolysis of 2,4-dinitrophenyl acetate (DNPA) can be used. A 50 mM solution of DNPA in ethanol is prepared and diluted fifty fold with 2 mM HCl. The other reactant is 1 M NaOH and the quencher is 2 M HCl. Initially, a sample of time equal to zero is obtained manually by mixing 1 mL of the DNPA solution with 5 mL of 2 M HCl and mixed well before adding 1 mL of 1 M NaOH and then make up to 10 mL with 2 M HCl. Then a time infinity sample is prepared by mixing 1 mL of DNPA with 1 mL of 1 M NaOH, allow a few seconds for the hydrolysis to occur and then making up to 10 mL with 2 M HCl. The absorbance spectra of both samples are then measured between 240 nm and 450 nm. It will be seen that a new shoulder occurs in the time infinity sample at about 294 nm and an isosbestic point (a wavelength at which two chemical species have the same molar extinction coefficient) is at 260 nm. The absorbances at both wavelengths are measured and the ratio A_{294nm}/A_{260nm} is calculated. Having made these measurements on the zero and infinity time points of the reaction, equal volumes of the DNPA and 1 M NaOH are mixed together in a quenched flow instrument and quenched with 2 M HCl with points taken over the time range of 0 to 150 msec. By measuring the A_{294nm}/A_{260nm} ratio of each quenched sample, the extent of the reaction is calculated. The data are then fitted to a single exponential. The fitted line should pass through zero time and an end point of 100% reaction. In addition, it should follow the same time course as when the DNPA solution is mixed with 1 M NaOH in a stopped-flow instrument with the absorbance being monitored at 420 nm.

In the case of temperature jump the most important parameters to be determined are 1) the rise time of the heating pulse, 2) the magnitude of the temperature increase, and 3) the cooling characteristics of the cell (see section IV.B.1). These can easily be determined by performing temperature jumps on a solution of a pH indicator such as phenolphthalein at a pH close to its pK_a.

B. Instrument settings

Several important factors must be considered in choosing the appropriate instrument settings for optical methods and these are discussed briefly here, with particular emphasis on fluorescence methods..

a. **Lamp selection**. Fluorescence measurements generally require high intensity light sources such as mercury, xenon, or xenon/mercury arc lamps. Xenon arc lamps have a relatively smooth emission spectrum whereas xenon or xenon/mercury lamps have a series of intense emission bands, which can sometimes be used to advantage. The emission from deuterium or quartz halide lamps is significantly less intense but is also less noisy. These lamps are frequently used in absorbance measurements and can sometimes be used for fluorescence excitation in the visible region if the fluorophore has a high quantum yield and extinction coefficient (Note: fluorescence intensity is proportional to the product of the quantum yield and the extinction coefficient).

b. **Slit widths**. Selection of slit widths is a balance between light intensity and spectral purity. If the fluorophore has a large Stokes shift (the wavelength difference between the excitation and emission maxima) a large slit width can be used to increase the light intensity. If the Stokes shift is small then the slit width may have to be reduced in order to exclude scattered light from the photomultiplier. Alternatively, the wavelength of the exciting light may be set to a shorter wavelength than the excitation maximum. These choices need to be made in conjunction with the choice of detection conditions. In some cases, slit widths may also need to be reduced to minimize photobleaching of the fluorophore. Photobleaching is not usually a problem on time scales of < 1 sec and can be quantified by mixing the fluorophore with buffer and recording the decrease in fluorescence intensity caused by the photobleaching.

c. **Detection of emission**. The emitted light is generally detected by a photomultiplier after it has passed through a suitable optical filter that should be selected to pass fluorescence emission light and exclude any exciting light that might be scattered by the solution. Scattered light arises from three sources: Rayleigh scattering of the exciting light (observed at the excitation wavelength λ_{Ex}), Rayleigh scattering of the first harmonic of the exciting light (observed at 2 x λ_{Ex}), and Raman scattering from the water. The wavelength (in nanometers) of the Raman scattering peak (λ_R) depends on the excitation wavelength according to $1/\lambda_R = 1/\lambda_{Ex} - 0.00034$. Filters should be chosen to maximize the fluorescence signal and minimize these other signals. This can be done using the appropriate cut-off and/or band pass filters. The other equally important issue is that one should maximize the signal change relative to the total background intensity in a rapid kinetic experiment. For this reason it is essential that a steady state investigation of the optical signal changes is used to determine the appropriate choice of emission filters.

d. **Selection of time constant**. The signal to noise ratio (S/N) in a rapid kinetic measurement is proportional to the square root of the instrumental time constant. In general, the time constant should be selected to be < 10% of the half time of the fastest process being observed. This gives the biggest reduction in noise without affecting the rate of the process being observed. In some instruments the noise can also be reduced by collecting data at the fastest possible rate and averaging appropriate blocks of data to give the individual time points.

e. **Recording and analyzing kinetic transients**. In the simplest cases data are usually collected using linear time scales. In more complex systems the observable processes may occur on very different time scales and it is then generally more appropriate to collect data with a logarithmic time base which allows data to be collected at progressively longer time intervals as the reaction proceeds (see Eccleston et al., 2001). Although the time constant will need to be set to be less than the fastest process the data can often be collected in the oversampling mode to improve the signal noise ratio for long time points. Although most stopped-flow fluorescence studies are performed at a single emission wavelength (or range of wavelengths selected by interference or band pass filters), it is also now possible to use rapid scanning monochromators or intensified diode array detectors to collect complete fluorescence spectra as a function of time.

   Analysis of the data obtained from rapid kinetic experiments by fitting one or more exponential terms to the curves obtained is usually straightforward in simple situations (see section VII). In this case the software supplied with commercially available equipment is often adequate. However, fitting to exponentials is not always the appropriate approach, for example, if second or higher order processes occur – see section VIII.

VI. Probes

In most cases an essential prerequisite for a successful rapid kinetic study is that there should be a suitable change in some optical signal, generally either absorbance or fluorescence, accompanying the reaction. The ideal case is, of course, where the optical signal is intrinsic to the system. There are, however, several approaches that may be used when there is no suitable change in an intrinsic signal, and these are the major topic of this section.

A. Intrinsic probes

Tryptophan is the major contributor to both the absorption and fluorescence properties of proteins and large changes, particularly in fluorescence, may accompany protein ligand interactions. Although tryptophan does have unique advantages as an intrinsic probe, it can be difficult to use for studying protein-nucleic acid interactions because the absorption spectra of the nucleic acids completely overlap that of tryptophan. It may also be difficult to use in the

study of protein-protein interactions because many proteins contain more than one tryptophan and the overall signal change accompanying the interaction can then be small. In certain cases it may be possible to use site-directed mutagenesis to replace some of tryptophan residues and thereby increase the size of the signal change (Málnási-Csizmadia et al., 2001, Wakelin et al., 2003). However, this procedure may, of course, alter the structure and/or function of the protein. Intrinsic optical signals associated with nucleic acids are generally much less useful in rapid kinetic studies, although major changes in the circular dichroism signals of the nucleic acids may result from interactions with proteins.

There are also numerous naturally occurring chromophoric cofactors and coenzymes such as NADH and pyridoxal phosphate that provide useful optical signals for rapid kinetic studies.

B. Extrinsic probes

An extrinsic probe is most often introduced by covalent attachment of a suitable chromophoric probe to one of the reaction partners.

There is a very wide range of commercially available fluorescent probes that react with either thiol or amine groups in proteins and oligonucleotides. A comprehensive guide to fluorescent probes and suitable labeling procedures is available from (Molecular Probes, 2006). Thiol or amine groups can be incorporated in a chemically synthesized oligonucleotide. These groups can then be conjugated to a thiol-reactive or amine reactive fluorophore. Labeling proteins can be more problematic. If the protein contains more than a single site for the label it may be difficult to obtain a reproducible product. Even when only a single site is available for labeling this may be far from the binding site for the reaction partner, and not therefore report on the interaction. In the latter case it may still be possible to study the interaction using anisotropy measurements (see section VI.D). An alternative approach is to use genetic engineering to create a protein containing a single cysteine residue that can then be specifically labeled (Brune et al., 1998, Brune et al., 2001). In this case, knowledge of the secondary structure of the protein is invaluable because it permits the cysteine to be introduced at a position where the label would be expected to be perturbed by ligand binding. For all of these approaches, it is essential that the modified protein is fully characterized, ideally using a combination of mass spectrometry and limited proteolysis, and that the ratio of probe to protein should be determined. It should also be demonstrated that the modification does not affect any biological activity of the protein. Finally, equilibrium binding measurements should be performed to determine the affinity of the modified protein for the ligand and this should be compared with that of the native protein. This can be done using suitable competition or displacement experiments (Martin and Bayley, 2002).

Another possible approach that can be used with proteins is to replace particular tryptophan residues with analogues that have absorption spectra whose absorption maxima are shifted toward the red (i.e., long wavelength) end of the spectrum, for example 5-hydroxytryptophan and 7-azatryptophan (Ross et al., 1997). The major experimental advantage of this approach

is that the red-shifted absorption spectrum allows selective excitation of the fluorescence of the analogue-containing protein in the presence of nucleic acids or other tryptophan-containing proteins. There are also highly fluorescent analogs of nucleotide bases, such as 2-amino-purine, that may provide correspondingly sensitive probes for studying the dynamics of protein-nucleic acid interactions (Hill and Royer, 1997). These analogs can be incorporated site-specifically into oligonucleotides using standard automated synthetic methods. A major advantage of using such analogues is their similarity in constitution and chemical properties to the natural compounds. Unlike large chromophores (see below), incorporation of these analogs into proteins or nucleic acids can normally be accomplished without introducing significant structural or chemical changes that might alter the measurement. It should not, however, be assumed that this is always the case.

Modification of the smaller reaction partner, such as a cofactor or other ligand for a protein, is attractive for two reasons. First because it will generally be much easier to produce a well-characterized product, and second because the fluorophore will necessarily be closer to the site of action. For example, many ribose modified derivatives of ATP and GTP have been synthesized to study the kinetic mechanisms of ATPases and GTPases (Jameson and Eccleston, 1997, Cremo, 2003). One potential disadvantage is that the properties of the labeled compound may differ significantly from those of the unlabelled one. For example, the 2'(3')-*O*-(*N*-methylanthraniloyl)-derivative of ADP binds to myosin subfragment 1 ten times more tightly than does ADP (Woodward et al., 1991). However, their fundamental mode of action is likely to remain the same as the parent nucleotide and they also remain useful for studying the unlabelled nucleotide by the use of competition and displacement experiments (see below).

C. Indicators, linked assays, and biosensors

There are numerous applications in which a reaction may be monitored by linking it to a second process that provides the appropriate spectroscopic signal. The essential requirement is that the linked process is very much faster than the one being studied, so that it does not affect the rate of the process being investigated. The simplest example is in the use of pH indicators to monitor reactions in which protons are either taken up or released. There are also several indicators available for Ca^{2+} and other metal ions (see Molecular Probes, 2006). Classical linked-enzyme assays are generally not fast enough for monitoring fast reactions but can be used to monitor those reactions occurring with sufficiently long half times. For example, the release of ADP can be monitored by linking it to the pyruvate kinase and lactate dehydrogenase system in which the conversion of NADH to NAD provides the optical signal (either fluorescence or absorbance). The last decade has seen the development of a large number of biosensors for studying rapid reactions. For example, Webb and colleagues have produced sensors for phosphate and purine nucleoside diphosphates by fluorescently labeling a phosphate binding protein (Brune et al., 1988) and a nucleoside diphosphate kinase (Brune, et al., 2001), respectively.

Use can also be made or resonance energy transfer if a suitable donor/emission pair is available with a combination of intrinsic and/or extrinsic fluorophores. The emission spectrum of tryptophan overlaps the excitation spectrum of 2'(3')-*O*-(*N*-methylanthraniloyl)-adenine nucleotides and this has been taken advantage of in stopped-flow studies of the myosin subfragment 1 ATPase mechanism (Woodward, et al., 1991). By exciting the tryptophan at 280 nm and observing the methylanthraniloyl emission, the bound fluorophore is preferentially excited over free fluorophore. This allows higher concentrations of the excess fluorophore to be used compared to exciting the methylanthraniloyl directly.

D. Fluorescence anisotropy

Fluorescence anisotropy measurements may be used to monitor reactions in which there is no change in fluorescence intensity. In these measurements the fluorophore is excited with vertically polarized light, and the intensity of the emitted light polarized parallel ($I_{//}$) and perpendicular ($I_{\perp}$) to the plane of the exciting light is recorded. The total fluorescence intensity is given by $I_{//} + 2\ I_{\perp}$ and the anisotropy is calculated as $r = (I_{//} - I_{\perp})/(I_{//} + 2\ I_{\perp})$. The anisotropy is related to fluorophore's rotational correlation time (τ_c) by the equation $r = r_o/(1 + \tau/\tau_c)$, where r_o is the limiting anisotropy of the fluorophore and τ is its excited state lifetime. Anisotropy measurements are particularly appropriate in the study of the binding of small fluorescent ligands to large macromolecules because τ_c is related to size and such reactions will therefore be accompanied by large increases in anisotropy. However, because anisotropy can be measured with high precision it is also possible to use this approach in the study of protein-protein interactions.

Measurements of anisotropy require an instrument that is equipped with a polarizer filter in the excitation path that can be rotated to give light polarized either vertical or horizontal to the laboratory axis. It is generally best to make the measurements in what is known as the "T" format, with two detection photomultipliers equipped with polarizers positioned at right angles to the incident light direction being used to measure $I_{//}$ and $I_{\perp}$. Because the two photomultipliers will respond differently to the parallel and perpendicular light they must be normalized. This is done by exciting the fluorophore with horizontally polarized light. Because the amount of light depolarized to either the parallel or perpendicular planes should be equal the high voltage on each photomultiplier must adjusted to give the same output signal. Methods for the analysis of anisotropy data are discussed in section VII.D.

VII. Experimental design and data analysis

In this section, we shall concentrate mainly on the determination of rate constants in reversible second-order processes, as introduced in Section III.B. Many protein-ligand and protein-protein interactions are of this type. It is invariably true that knowledge of the equilibrium dissociation constant K_d (k_-/k_+) is helpful in designing transient kinetic experiments and in interpreting the data obtained from them. Methods for determining these constants are

described elsewhere in this volume and in several published reviews (for example, Eftink, 1997).

A. General considerations

1. Flow Methods

Stopped-flow kinetic studies of reactions of the type shown in Scheme **II** are generally performed under pseudo first-order conditions, i.e., with one of the reagents (X) in large excess over the other (see Section III.B.1). As $k_{OBS} = k_{+}X_{tot} + k_{-}$ (equation 5), k_{OBS} must determined from experimental transients recorded at several different values of *Xtot*. A plot of k_{OBS} *versus* X_0 should then be linear with slope k_{+1} and intercept k_{-1}, provided the binding is indeed a simple second order process.

As noted above, it is important in transient kinetic experiments that one should maximize the ratio of signal change to total background signal. Thus, for example, if the ligand (L) and the complex (PL) are fluorescent, but the protein is not, then the protein should be the component used in excess. In the ideal case the concentration of the reagent in excess should be at least ten-fold higher than the other. If lower ratios are used, the measured value of k_{OBS} will be significantly different from than that predicted by Equation 5.

It is clearly important that the largest possible concentration range should be covered in experiments of this type. This permits accurate determination of the kinetic constants, and the demonstration that k_{OBS} varies linearly over an extended concentration range is necessary to confirm that Scheme **II** is an adequate description of the process. Consider, for example, the case where the protein is the reactant used in excess. In a typical situation with an association rate constant of the order of 10^7 $M^{-1}s^{-1}$, a dissociation rate constant of 10 s^{-1}, and an instrument dead time of 2 ms, the largest usable value of P_{tot}, the total concentration of P, would be about 50 μM (k_{OBS} = 510 s^{-1}). The lower concentration limit is determined by the lowest concentration of ligand that can be used whilst still maintaining the relationship $P_{tot} \gg L_{tot}$ (L_{tot} is the total concentration of L). As the ligand concentration is decreased, the photomultiplier gain will have to be increased, and at some point this will result in an unacceptably high noise level. In the case of low affinity interactions, where the dissociation rate constant (k_{-1}) is likely to be large, it may be possible to cover only a limited concentration range before k_{obs} becomes too fast to measure. In such cases it is generally possible to extend the available range by performing the experiment at a lower temperature. In cases where the association rate constant cannot be accurately determined, it can be estimated from the measured dissociation rate constant and a known dissociation constant using $k_{+1} = k_{-1}/K_d$. This is, of course, only true if the reaction conforms to Scheme **II**. Figure **2** illustrates under which conditions k_{+1} and k_{-1} can be determined accurately from this type of experiment.

The measured values of the rate constants should be used to calculate a value for the K_d for the interaction using the relationship $K_d = k_{-1}/k_{+1}$ and this should agree with the K_d determined

from equilibrium titrations. A significant difference between the values may indicate that Scheme **II** is not an adequate description of the process. The observed reaction amplitudes should also be shown to be consistent with the K_d measured independently. The concentration of protein-ligand complex formed following stopped-flow mixing is, of course, readily calculated from the total concentrations of protein and ligand present *after* mixing and the known K_d using:

$$[PL] = \frac{(P_{tot} + L_{tot} + K_d) - \sqrt{(P_{tot} + L_{tot} + K_d)^2 - 4P_{tot}L_{tot}]}}{2} \quad (7)$$

2. Relaxation experiments

a. Relaxation times. In the case of a relaxation measurement, such as temperature jump, analysis of the observed exponential time course gives the relaxation time τ, which depends on the concentrations of P and L according to equation 6 ($\tau^{-1} = k_{+1}([P]+[L]) + k_{-1}$). Note [P] and [L] are the concentrations of free protein and free ligand present at equilibrium *prior* to application of the temperature jump, whereas the rate constants are those for the temperature reached *after* the temperature jump. A plot of the reciprocal relaxation time *versus* ([P] + [L]) should be linear with slope k_{+1} and intercept k_{-1}. The values of ([*P*] + [*L*]) can be calculated from the known total concentrations (P_{tot} and L_{tot}) and an experimentally determined overall dissociation constant K_d (= k_{-1}/k_{+1}) using Equation 7. There may, however, be instances where it is not possible to determine an accurate value of the dissociation constant and [P] and [L] cannot then be calculated. There are three ways around this problem

1. Use a large excess of one reagent (10-fold or greater) so that the sum of [*P*] and [*L*] is effectively equal to the total concentration of the reagent in excess. In order to maximize the ratio of signal change to background signal the reagent used in excess should be the one with the smallest contribution to the total optical signal. As with stopped-flow measurements a potential disadvantage of this method is that it may require the use of a low concentration of the component with the optical signal and this may result in unacceptably high noise levels. A further significant disadvantage is that that greatest perturbation of the equilibrium is achieved when the concentrations of protein and ligand are equal (see below)

2. Use the relationship

$$\tau^{-2} = 2k_{+1}k_{-1}([P_{tot}]+[L_{tot}]) + k_{-1}^2 \quad (8)$$

under conditions where the total concentrations of protein and ligand are the same (P_{tot} = L_{tot}). This method has the advantage that the largest perturbations of the equilibrium are obtained when P_{tot} = L_{tot}.(see below) It does, however, have two potential disadvantages. If there is an error in the estimation of either of the concentrations then $P_{tot} \neq L_{tot}$ and the plot will show upward curvature whose

magnitude will depend on the magnitude of the difference. Even relatively small curvature can, under certain conditions, result in large errors in the calculated dissociation rate constant. Given the difficulties of estimating protein concentrations this is quite a likely source of error. The other problem is that errors in the reciprocal relaxation time translate into larger errors in τ^{-2}.

3. Equations 7 and 8 can be combined to give a single equation describing the dependence of the reciprocal relaxation time on the *total* concentrations of the two reactants:

$$\tau^{-1} = k_{+1}\sqrt{(P_{tot} + L_{tot} + k_{-1}/k_{+1})^2 - 4P_{tot}L_{tot}} \tag{9}$$

b. Amplitudes. The magnitude of the concentration perturbation for the simple equilibrium shown in Scheme **II** is Δ[L], where $\Delta[L] = \Delta[P] = -\Delta[PL]$. For temperature jump experiments, it has been shown (Malcolm, 1972) that:

$$\Delta[L] = \alpha \cdot \delta \ln K_d = \alpha\left(\frac{-\Delta H}{RT^2}\right)\cdot \delta T \tag{10}$$

The amplitude of the observed relaxation process therefore depends on the enthalpy (ΔH), on the size of the temperature jump (dT)?and on the magnitude of α, which is given by:

$$a = -0.5K_d + 0.5K_d\sqrt{1 - 4\left(\frac{S}{K_d + S}\right)^2\left(\frac{b}{(1+b)^2}\right)} \tag{11}$$

where $S = P_{tot} + L_{tot}$ and $\beta = P_{tot}/L_{tot}$. When the term after the minus sign in the square root term is small this expression may be simplified (Malcolm, 1972) to:

$$a = K_d\left(\frac{S}{K_d + S}\right)^2\left(\frac{b}{(1+b)^2}\right) \tag{12}$$

The term $\beta/(1+\beta)^2$ has a maximum when $\beta = 1$. Therefore, the magnitude of β, and hence the total observed amplitude, increases as *S* increases and as β approaches one. This is illustrated in Figure **3**. In cases where the affinity is reduced at lower pH values, it is possible to produce larger perturbations by using a buffer such as Tris, which has a high temperature coefficient.

B. Displacement experiments

Small dissociation rate constants may not be well determined using the above approaches because the intercept will be very close to the origin (see Figure **2**). Stopped-flow methods can sometimes be used to make an independent measurement of the dissociation rate constant if a displacement experiment can be performed. For example, an excess of a non-

fluorescent ligand (N) can be used to dissociate a fluorescent ligand (L) from its complex with the protein. The relevant reactions are:

[SCHEME **III** HERE]

The experiment involves rapidly mixing one solution containing P *and* L (at concentrations chosen to give a reasonable saturation of P) with a second solution containing an excess of N. High concentrations of N are required so that when L dissociates from the protein it cannot re-associate before N binds. The rate constant of the observed process should then be equal to k_{-1}. However, depending on the relative values of the other rate constants this may not always be the case, and the observed rate may be either higher or lower than the true dissociation rate constant (see Wu et al., 1992). To confirm that the true dissociation rate constant is being measured it must be demonstrated that the observed rate is independent of the concentration of the displacing ligand, N. If the observed rate does vary with the concentration of N then the observed rate will plateau at the true value of k_{-1} at sufficiently high [*N*]. Wu et al. (1992) have also described ways in which the truly dissociative mechanism represented by Scheme **III** (L must dissociate before N binds) can be distinguished from an associative mechanism in which a ternary complex is formed between the incoming ligand (N) and the complex containing the leaving ligand (PL) prior to dissociation of L. In the associative mechanism the observed rate will also generally plateau at high [*N*] but in most cases this value will be higher than k_{-1}.

In some cases it is also possible to use displacement experiments to determine dissociation rate constants for an optically silent ligand by using a fluorescent (or absorbing) ligand to induce the displacement. This may, however, be technically difficult because the strong fluorescent background will result in poor S/N ratios.

Dissociation of a protein-ligand complex can, in certain cases, be induced by rapid mixing with an excess of a compound that reacts with the ligand rather than the protein. For example, the dissociation of calcium from calcium binding proteins such as calmodulin and calbindin D_{9k} can be studied by rapid mixing with an excess of a fluorescent calcium chelator such as Quin 2 (Martin et al., 1990)), which forms a strongly fluorescing, high affinity 1:1 complex with calcium.

C. Competition experiments

The interaction of a non-fluorescent ligand with a protein can, in certain cases, be studied using competition with a second fluorescent ligand. The reactions involved are again those shown in Scheme **III**. The experiment involves rapidly mixing the protein with different premixed solutions of N *and* L. If the dissociation rate constants are very small and both L and N are in large excess over P then the observed first-order rate constant will be given by:

$$k_{OBS} = k_{+1}L_{tot} + k_{+2}N_{tot} \qquad (13)$$

If the experiment is performed using different concentrations of N at a fixed concentration of L then a plot of k_{OBS} versus [N_{tot}] should then give a straight line with slope k_{+2} and intercept $k_{+1}L_{tot}$. More complex behavior will be observed if the dissociation rate constants are not small enough to be ignored. Competition experiments can also be used, even if one of the reactions consists of two steps (e.g. as in scheme **IV**, (Engelborghs and Fitzgerald, 1987)).

Competition experiments can also be performed using relaxation measurements. If conditions are chosen such that the reaction with the fluorescent ligand is much faster than the reaction with the non-fluorescent ligand then two relaxation processes will be observed. The reciprocal relaxation times for the fast (τ_F) and slow (τ_S) processes will be given by (Guillain and Thusius, 1970):

$$\tau_F^{-1} = k_{+1}([P]+[L]+k_{-1}) \tag{14}$$

$$\tau_S^{-1} = k_{+2}\left([P]+\frac{[N]([P]+K_{dl})}{[P]+[L]+K_{dl}}\right)+k_{-2} \tag{15}$$

One of the potential advantages of relaxation methods over flow methods is that such expressions for relaxation times are generally much easier to derive than the rate expressions for stopped-flow measurements and the experiments do not have to be performed under fixed (e.g., pseudo first-order) conditions. The major disadvantage is that accurate equilibrium measurements must be done to permit calculation of the equilibrium concentrations. For this particular example it should be possible to determine K_{d1} by direct equilibrium titration and K_{d2} by a displacement titration in which N is used to displace L from a preformed PL complex (see Martin and Bayley, 2002).

D. Analysis of stopped-flow anisotropy data

If there is no change in intensity accompanying complex formation then the kinetic transients can be analyzed as simple exponentials and the data plotted using Equation 5. However, if there is a change in fluorescence intensity then the time-dependent change in anisotropy must be described by (Eccleston, et al., 2001):

$$r(t) = f_L(t)r_L + f_{PL}(t)r_{PL} \tag{16}$$

where r_L and r_{PL} are the anisotropies of *L* and *P*, and $f_L(t)$ and $f_{PL}(t)$ are the fractional intensities of light coming from *L* and *PL* at time *t*:

$$f_L(t) = \frac{[L](t)}{[L](t)+D[PL](t)} \text{ and } f_{PL}(t) = 1-f_L(t)$$

Here *D* is the fluorescence intensity of *PL* divided by that of *L*. Substituting in Equation 16 gives:

$$r(t) = \frac{[L](t)(r_L - r_{PL})}{[L](t) + D[PL](t)} + r_{PL}$$

Substituting the expressions for the disappearance of *L* and appearance of *PL*

$[L](t) = [L_0]e^{-k_{OBS}t}$ and $[PL](t) = [L_0] - [L](t)$ gives the expression that must be used to analyze the time dependence of the anisotropy change in order to obtain k_{OBS}:

$$r(t) = \frac{(r_L - r_{PL})}{1 - D + De^{k_{OBS}t}} \quad (17)$$

VIII. Complex reactions

A. Two-step mechanisms

Although many protein ligand interactions conform to Scheme **II** this is by no means always the case. The most obvious indication of additional complexity in a rapid kinetic investigation is the observation of more than a single kinetic phase. When only a single kinetic phase is observed complexity will most likely be indicated by the observation that the variation of the observed rate with concentration is not linear. One of the most commonly encountered complexities is the presence of an additional step that involves an isomerization. This can be a first-order isomerization of a protein-ligand complex following an initial second-order binding event:

[SCHEME **IV** HERE]

or a first-order isomerization of the protein (or the ligand) followed by a second-order binding event.

[SCHEME **V** HERE]

It is important to realize that neither of these schemes would be identified by simple equilibrium binding measurements. Analysis of binding curves for these schemes will always appear to conform to Scheme **II** with the experimentally measured dissociation constant given by:

$$K_d = \frac{K_{d1}K_{d2}}{1 + K_{d2}} \text{ for Scheme } \mathbf{IV} \quad (18)$$

and

$$K_d = K_{d2}(1 + K_{d1}) \text{ for Scheme } \mathbf{V} \quad (19)$$

with the individual equilibrium dissociation constants defined as $K_{d1} = k_{-1}/k_{+1}$ and $K_{d2} = k_{-2}/k_{+2}$ for both schemes.

1. Flow methods

The analytical solutions to the rate equations for these simple two-step mechanisms can only be derived for flow experiments when one of the concentrations is in large excess, so that it remains effectively invariant over the time-course of the reaction. If the second-order binding step in Scheme **IV** is very much faster than the isomerization step, and L is in large excess over P, then a stopped-flow record will have two kinetic phases, with the fast process varying linearly with L_{tot} according to (Halford, 1971):

$$k_{OBS}(F) = k_{+1}L_{tot} + k_{-1} \tag{20}$$

and the slow process varying hyperbolically with L_{tot} according to:

$$k_{OBS}(S) = \frac{k_{+2}L_{tot}}{K_{d1} + L_{tot}} + k_{-2} \tag{21}$$

What will actually be observed experimentally will clearly depend on the relative contributions of the different species to the optical signal being monitored, as well as on the magnitudes of the individual rate constants (see Figure **4**). Only in the most favorable cases where two easily resolvable kinetic events are observed over a wide range of L_{tot} values (with the bimolecular step *always* remaining very much faster than the isomerization for all L_{tot}) will it be possible to extract all four rate constants by analyzing Equations 20 and 21. Thus, although inspection of Equation 21 shows that $k_{OBS}(S)$ should *increase* from k_{-2} when $L_{tot} << K_{d1}$ to $(k_{-2} + k_{+2})$ when $L_{tot} >> K_{d1}$ this will not always be observable. Consider, for example, a typical situation where the bimolecular rate constant (k_{+1}) is 10^7 $M^{-1}s^{-1}$ and the overall equilibrium dissociation constant as defined in Equation 18 is 0.1 µM. Two extreme situations can then be considered:

- If K_{d1} is low then given the nature of the typical stopped-flow experiment it is unlikely that it will be possible to work under conditions where $L_{tot} << K_{d1}$ and $k_{OBS}(S)$ will only vary significantly with L_{tot} when $k_{-2} < k_{+2}$ and k_{-2} will generally be difficult to determine. In extreme cases K_{d1} may be so low that $k_{OBS}(S)$ may well be completely independent of L_{tot} under all attainable experimental conditions and only the sum of the rate constants for the isomerization step will be measurable. In such cases it may be possible to perform displacement experiments (see section VII.B) in order to determine one or both of the dissociation rate constants.

- If, on the other hand, the bimolecular step is the fast diffusion controlled formation of an encounter complex with very low overall affinity (high K_{d1} ~ 1 mM) then the value of K_{d2} would need to be 100 µM to give the overall equilibrium dissociation constant of 0.1 µM (see Equation 18). A typical stopped-flow experiment could then show only a single transient process because occupancy of the intermediate PL would always be very low. The single observed rate might then vary linearly with L_{tot} (since

deviations from linearity would only be observed when L_{tot} approached K_{d1}, see Equation 21) with an apparent second-order rate constant of k_{+2}/K_{d1} and dissociation rate constant k_{-2}. When L_{tot} does approach K_{d1}, some curvature may, of course, be observed and the *initial* slope can then be taken as equal to k_{+2}/K_{d1} (see (De La Cruz et al., 2001) for a good discussion of these effects).

The association rate constants measured for protein-ligand and protein-protein interactions are, in fact, often significantly lower than the values predicted using theoretical calculations based on diffusion coefficients, shape, and viscosity. Scheme **IV** with a high value of K_{d1} and a low value of k_{+2} is frequently invoked as an explanation for the observation of these unexpectedly low values.

In the case of Scheme **V**, with the bimolecular step very much faster than the isomerisation step, the rate expressions for experiments performed under the condition that $L_{tot} > (P_{tot} + P^*_{tot})$ are (Halford, 1971):

$$k_{OBS}(F) = k_{+2}L_{tot} + k_{-2} \tag{22}$$

$$k_{OBS}(S) = \frac{k_{-1}K_{d2}}{K_{d2} + L_{tot}} + k_{+1} \tag{23}$$

Thus, scheme **V** can, at least in principle, be distinguished from Scheme **IV** by the fact that the observed rate for the slow process should *decrease* from $(k_{-1} + k_{+1})$ when $L_{tot} \ll K_{d2}$ to k_{+1} when $L_{tot} \gg K_{d2}$. However, as for scheme **IV**, only in the most favorable cases will it be possible to extract all four rate constants for the reaction.

2. Relaxation methods

The relaxation times in a multi-step process are the eigen values of a system of coupled differential equations. There will be as many relaxations as there are *independent* concentration variables, though not all of these relaxations will necessarily be observable. The number of independent concentration variables (two for schemes **IV** and **V**) will be equal to or smaller than the number of steps, depending on the concentration conservation conditions for the scheme. For scheme **IV**, Eigen (1968) has shown that the sums and products of the reciprocal relaxation times are given by:

$$\tau_F^{-1} + \tau_S^{-1} = k_{+1}[P] + [L] + k_{-1} + k_{+2} + k_{-2} \tag{24}$$

$$\tau_F^{-1}\tau_S^{-1} = k_{+1}(k_{+2} + k_{-2})([P] + [L]) + k_{-1} + k_{-1}k_{-2} \tag{25}$$

and in favorable cases these two combinations can be plotted *versus* ([*P*]+[*L*]) to yield all four rate constants (Eigen, 1968). If the relaxation times are sufficiently well separated, these equations can be uncoupled to relate the individual relaxation times to particular steps. For example, if the first (bimolecular) step in Scheme **IV** is very much faster than the isomerization step then it can be treated as an isolated process (namely Scheme **II**), but an

additional concentration factor has to be included with the isomerization term to account for coupling with the faster step.

Thus, because $k_{+1}([P]+[L]) + k_{-1} >> k_{+2} + k_{-2}$, one can write (Halford, 1972):

$$\tau_F^{-1} = k_{+1}[P]+[L]+k_{-1} \tag{26}$$

and

$$\tau_S^{-1} = \frac{\tau_F^{-1}\tau_S^{-1}}{k_{+1}([P]+[L])+k_{-1}} = \frac{k_{+2}([P]+[L])}{[P]+[L]+K_{dl}} + k_{-2} \tag{27}$$

The reciprocal relaxation time will then vary from k_{-2} when ($[P]+[L]$) << K_{d1} to a limiting plateau value of $k_{+2} + k_{-2}$ when ($[P]+[L]$) >> K_{d1}. As with flow experiments it may not always be possible to work under conditions that permit determination of all four rate constants.

For scheme **V** with a fast bimolecular step, uncoupling leads to the following expressions for the relaxation times:

$$\frac{1}{\tau_F} = k_{+2}([P^*]+[L]) + k_{-2} \tag{28}$$

$$\frac{1}{\tau_S} = \frac{k_{-2}([P^*]+K_{d2})}{[P^*]+[L]+K_{d2}} + k_{-2} \tag{29}$$

In the case of Scheme **IV**, solving Equation 7 using the measured overall dissociation constant gives ([PL] + [PL*]), so that [P] and [L] for use in Equations 26 and 27 can be calculated. This is not the case for scheme **V**; solving Equation 7 gives [PL*] but the equilibrium between P and P* is not known and [P*] cannot be calculated. Two solutions are possible: work under conditions where L is in large excess or use an iterative procedure in the fitting.

B. Multi-step mechanisms

Multi-step mechanisms will almost invariably consist of a series of first- and second-order reactions and in some simple cases, particularly for relaxation experiments, it is possible to derive the analytical solutions necessary for a kinetic analysis (see, for example, Halford, 1972). However, a more common approach is to try to study the individual steps in isolation (for example, De La Cruz et al., 1999, De La Cruz, et al., 2001, Eccleston et al., 2006).

IX. Data and analysis

As noted above, most commercial equipment will come with software for analysing kinetic transients as sums of exponential terms and this aspect of data analysis will not be discussed further here. When analysing rate expressions such as that given in Equation 23 it is, in general, not good practice to transform them into linear functions, because the associated

errors transform accordingly. There are now numerous mathematical procedures available for χ^2-minimization of non-linear functions such as these; for example, the widely used Marquardt procedure is both efficient and relatively robust (Press et al., 1990). Whenever possible, it is best to determine the variance in k_{OBS} values for each value of the independent concentration variable. The resulting sample variances may then be used to weight each k_{OBS} value by the inverse of its estimated variance. In some cases it may not be possible to obtain variances for individual samples, and it is then reasonable to assume that the *relative* error in k_{OBS} is constant. The fitting should then be done to the logarithm of k_{OBS}, since the error in $\log(k_{OBS})$ will be constant. This is particularly important in cases where k_{OBS} values vary by more than an order of magnitude.

As noted elsewhere, most stopped-flow fluorescence studies are performed at a single emission wavelength (or range of wavelengths), but it is also possible to collect complete fluorescence spectra as a function of time. This permits a more rigorous analysis of kinetic data and allows the measurement of the spectra of intermediates in the reaction pathway. Furthermore, the application of principal component analysis may permit the direct determination of the number of fluorescing species in the reaction scheme on a completely model-independent basis, and therefore may aid in model selection.

The traditional approaches to analysing rapid kinetic data described in the previous sections generally involve fitting the time dependence of an observed optical signal to one or more exponential terms. The requirement for an explicit analytical solution to the rate equations for the reaction generally necessitates simplifying assumptions and places what are often severe constraints on the experimental conditions that can be used. In many cases, it will not be possible to work within these constraints. For example, if it is not possible to work under pseudo first-order conditions, it will be necessary to analyse progress curves for two-step reactions using an iterative method based on numerical integration of the appropriate differential rate equations.

Global analysis allows the fitting of multiple kinetic data sets obtained under different concentration conditions. The simultaneous analysis of the different data sets has the potential to achieve better definition of the rate constants common to all the sets. In favourable cases it may allow the determination of kinetic constants not attainable by traditional methods and can be used to distinguish between different kinetic models. Another strong point of global analysis is that the different data sets can be obtained using different methods, e.g., fluorescence intensity and anisotropy data, in which the kinetic constants are nevertheless the same. In such cases it is important to weight the different data sets correctly. This can be done by determining the standard deviation for a signal that has reached equilibrium. One potential drawback is that if the kinetic constants to be determined are not adequately constrained by the data there will be a large range of constants giving equally good fits to the data. The extent to which a particular rate constant is defined by the data can be tested by simulating the mechanism and varying each rate constant in turn (Schilstra et al,

this volume). Rate constants that are poorly constrained may need to be held constant, either at an estimated value or at a value determined in an independent approach. We recommend that a conventional kinetic analysis should always be attempted before embarking on global analysis. No mathematical treatment, however sophisticated, can make up for less than adequate data collection.

Having extracted rate constants it is generally instructive to simulate the reaction by computer methods (see Schilstra et al., this volume) in order to see how well the data fits the assumed mechanism. This is most often done at the level of simulating how the observed rate of a particular process depends upon the concentrations of the reagents but it is also instructive to simulate individual reaction traces. Computer simulation is also invaluable as a teaching tool and a useful aid in the design of experiments. In our experience, intuitive arguments can frequently be wrong, even in apparently simple situations.

References

Abbruzzetti, S., Crema, E., Masino, L., Vecli, A., Viappiani, C., Small, J.R., Libertini, L.J., and Small, E.W. (2000). Fast Events in Protein Folding: Structural Volume Changes Accompanying the Early Events in the Nright-arrowI Transition of Apomyoglobin Induced by Ultrafast pH Jump. *Biophys. J.* 78**,** 405-415.

Brune, M., Corrie, J.E.T., and Webb, M.R. (2001). A fluorescent sensor of the phosphorylation state of nucleoside diphosphate kinase and its use to monitor nucleoside diphosphate concentrations in real time. *Biochemistry* 40**,** 5087-5094.

Brune, M., Hunter, J.L., Howell, S.A., Martin, S.R., Hazlett, T.L., Corrie, J.E.T., and Webb, M.R. (1988). Mechanism of inorganic phosphate interaction with phosphate binding protein from *Escherichia coli*. *Biochemistry* 37**,** 10370-10380.

Brune, M., Hunter, J.L., Howell, S.A., Martin, S.R., Hazlett, T.L., Corrie, J.E.T., and Webb, M.R. (1998). Mechanism of inorganic phosphate interaction with phosphate binding protein from *Escherichia coli*. *Biochemistry* 37**,** 10370-10380.

Caldin, E.F. (1964). "Fast reactions in Solution", Blackwell Scientific Publications, Oxford.

Cremo, R.C. (2003). Fluorescent nucleotides: synthesis and characterization. *Methods Enzymol.* 360**,** 128–177.

De La Cruz, E.M., Ostap, E.M., and Sweeney, H.L. (2001). Kinetic Mechanism and Regulation of Myosin VI. *J. Biol. Chem.* 276**,** 32373-32381.

De La Cruz, E.M., Wells, A.L., Rosenfeld, S.S., Ostap, E.M., and Sweeney, H.L. (1999). The kinetic mechanism of myosin V. *PNAS* 96**,** 13726-13731.

Eccleston, J.F., Hutchinson, J.P., and White, H.D. (2001) *in* "Protein-ligand interactions: Structure and spectroscopy" (S.E. Harding, and B.Z. Chowdhry, Eds.), pp. 201-237, Oxford University Press, Oxford.

Eccleston, J.F., Petrovic, A., Davis, C.T., Rangachari, K., and Wilson, R.J.M. (2006). The Kinetic Mechanism of the SufC ATPase: the cleavage step is accelerated by SufB. *J. Biol. Chem.* 281**,** 8371-8378.

Eftink, M.R. (1997). Fluorescence methods for studying equilibrium macromolecule-ligand interactions. *Meth. Enzymol.* 278**,** 221-257.

Eigen, M. (1968). New looks and outlooks on physical enzymology. *Quart. Rev. Biophys.* 1**,** 3-33.

Engelborghs, Y., and Fitzgerald, T.J. (1987). A fluorescence stopped flow study of the competition and displacement kinetics of podophyllotoxin and the colchicine analog 2-methoxy-5-(2',3',4'-trimethoxyphenyl) tropone on tubulin. *J. Biol. Chem.* 262**,** 5204-5209.

Guillain, F., and Thusius, D. (1970). The use of proflavin as an indicator in temperature-jump studies of the binding of a competitive inhibitor to trypsin. *J. Amer. Chem. Soc.* 92**,** 5534-5536.

Gutman, M., and Nachliel, E. (1990). The dynamic aspects of proton transfer processes. *Biochim. Biophys Acta* 1015**,** 391-414.

Halford, S.E. (1971). Escherichia coli alkaline phosphatase. An analysis of transient kinetics. *Biochem. J.* 125.

Halford, S.E. (1972). Escherichia coli alkaline phosphatase. Relaxation spectra of ligand binding. *Biochem. J.* 126**,** 727-738.

Hill, J.J., and Royer, C.A. (1997). Fluorescence approaches to the study of protein-nucleic acid complexation. *Meth. Enzymol.* 278**,** 390-416.

Jameson, D.M., and Eccleston, J.F. (1997). Fluorescent nucleotide analogs: synthesis and applications. *Meth. Enzymol.* 278**,** 363-390.

Malcolm, A.D. (1972). Coenzyme binding to glutamate dehydrogenase. A study by relaxation kinetics. *Eur. J. Biochem.* 27**,** 453-461.

Málnási-Csizmadia, A., Pearson, D.S., Kovács, M., Woolley, R.J., Geeves, M.A., and Bagshaw, C.R. (2001). Kinetic resolution of a conformational change and the ATP hydrolysis step using relaxation methods with a Dictyostelium myosin II mutant containing a single tryptophan residue. *Biochemistry* 40**,** 12727-12737.

Martin, S.R., and Bayley, P.M. (2002). Regulatory implications of a novel mode of interaction of calmodulin with a double IQ-motif target sequence from murine dilute myosin V. *Protein Science* 11**,** 2909-2923.

Martin, S.R., Linse, S., Johansson, C., Bayley, P.M., and Forsén, S. (1990). Protein surface charges and Ca^{2+} binding to individual sites in calbindin D_{9k}: Stopped flow studies. *Biochemistry* 29**,** 4188 4193.

Molecular Probes (2006). "The Handbook - A Guide to Fluorescent Probes and Labeling Technologies". Invitrogen, http://probes.invitrogen.com/handbook/.

Pearson, D.S., Holtermann, H., Ellison, P., Cremo, C., and Geeves, M.A. (2002). A novel pressure-jump apparatus for the microvolume analysis of protein-ligand and protein-protein interactions: its application to nucleotide binding to skeletal-muscle and smooth-muscle myosin subfragment-1. *Biochem. J.* 366**,** 643-651.

Press, W.H., Flannery, B.P., Teukolsky, B.P., and Vetterling, W.T. (1990). "Numerical recipes. The art of scientific computing. Fortran version." Cambridge University Press, Cambridge UK.

Rabl, C.R. (1979) *in* "Techniques and Applications of Fast Reactions in Solution" (W.J. Gettins, and E. Wyn-Jones, Eds.), pp. 77-82, Reidel, Dordrecht.

Ross, J.B.A., Szabo, A.G., and Hogue, C.W.V. (1997). Enhancement of protein spectra with tryptophan analogs: Fluorescence spectroscopy of protein-protein and protein-nucleic acid interactions. *Meth. Enzymol.* 278**,** 151-190.

Shastry, M.C.R., Luck, S.D., and Roder, H. (1998). A continuous-flow capillary mixer to monitor reactions on the microsecond time scale. *Biophys. J.* 74**,** 2714-2721.

Turner, D.H., Flynn, G.W., Sutin, N., and Beitz, J.V. (1972). Laser Raman temperature-jump study of the kinetics of the triiodide equilibrium. Relaxation times in the 10-8 -10-7 second range. *J. Am. Chem. Soc. USA* 94**,** 1554 - 1559.

Wakelin, S., Conibear, P.B., Woolley, R.J., Floyd, D.N., Bagshaw, C.R., Kovács, M., and Málnási-Csizmadia (2003). Engineering Dictyostelium discoideum myosin II for the introduction of site-specific fluorescence probes. *J. Musc. Res. Cell Motil.* 23**,** 673-683.

Williams, S., Causgrove, T.P., Gilmanshin, R., Fang, K.S., Callender, R.H., Woodruff, W.H., and Dyer, R.B. (1996). Fast Events in Protein Folding: Helix Melting and Formation in a Small Peptide. *Biochemistry* 35**,** 691-697.

Woodward, S.K.A., Eccleston, J.F., and Geeves, M.A. (1991). Kinetics of the interaction of 2'(3')-O-(N-methylanthraniloyl)-ATP with myosin subfragment 1 and actomyosin subfragment 1: Characterization of two acto.S1.ADP complexes. *Biochemistry* 30**,** 422 - 430.

Wu, X., Gutfreund, H., and Chock, P.B. (1992). Kinetic method for differentiating mechanisms for ligand exchange reactions: Application to test for substrate channeling in glycolysis. *Biochemistry* 31**,** 2123-2128.

Figure legends

Figure 1. Transient for the reaction P ⇔ P* (Scheme **I**). Values of k_{+1} and k_{-1} were 6 and 10 s^{-1}, unless otherwise indicated; the total concentration of P, P_{tot}, was 1 µM. a) Definition of P^*_0 and P^*_{eq} (initial and equilibrium concentrations of P*), $\Delta[P^*]$ (reaction amplitude), $t_{1/2}$ (half-life), and τ (relaxation time), which is equal to the reciprocal of k_{OBS} (observed rate). b) The relaxation time is equal to $1/k_{OBS} = 1/(k_{+1} + k_{-1})$ (62.5 ms for the rate constants used here), independent of the initial concentration of P* (0, 0.45, and 1 µM in curves A, B, and C, respectively). c) If two systems have equal forward rate constants the system with the largest reverse rate constant will reach equilibrium first (curves D (k_{+1} = 6; k_{OBS} = 16) and E (k_{+1} = 6; k_{OBS} = 6.1)), whereas two systems with identical equilibrium constants may have different observed rates (curves D (K = 0.6, k_{OBS} = 16) and F (K = 0.6, k_{OBS} = 8)).

Figure 2. Left panels: typical transients (simulated) in a set of stopped-flow experiments in which a fluorescent ligand L (at 1 µM) is mixed with a large excess (10 – 110 µM) of non-fluorescent protein P. The specific fluorescence of the complex PL is higher than that of L, so that the overall fluorescence of the mixture increases as the system approaches equilibrium. The vertical axis indicates the change in fluorescence observed as a percentage of the maximal change (the difference in fluorescence between 1 µM L and 1 µM PL). Right panels: plots of the observed rates obtained from the transients versus the concentration of the component in excess (P). As $k_{OBS} = k_{+1}[P] + k_{-1}$, the slope and intercept of these plots are k_{+1} and k_{-1}, respectively. a) both slope and intercept (1 $\mu M^{-1}s^{-1}$ and 10 s^{-1}, so that K_d = 10 µM) are well-defined (have small associated errors) under the experimental conditions; b) k_{+1} is well-defined (1 $\mu M^{-1}s^{-1}$) but k_{-1} is too small (because K_d = 1 µM) to be obtained with any accuracy. c) k_{-1} is well-defined (100 s^{-1}) but k_{+1} is very small (as K_d = 1 mM in this system). Note that the affinity of P for L is so low, that at 100 µM P, only about 10% of the total L has formed PL.

Figure 3. A set of transients (simulated) that might be observed in a temperature-jump experiment. A rapid temperature-jump (from 20 to 25 ºC) is applied to mixtures of P and L in which the sum of [*P*] and [*L*] is 20 µM, but their ratio varies. The right panel, in which the reaction amplitude $\Delta[PL]$ is plotted against [*P*], shows that the amplitude is maximal when [*P*]/[*L*] = 1.

Figure 4. Relationship between the simulated time dependent changes in concentrations of P, PL, and PL* (grey lines, right axis) for the reaction scheme P + L ⇔ PL ⇔ PL* (Scheme IV, with *Ptot* = 1 µM, *Ltot* = 10 µM, k_{+1} = 10 $\mu M^{-1}s^{-1}$, and k_{-1}, k_{+2}, k_{-1} = 10, 5, and 1 s^{-1}, respectively) and the observed fluorescence of the mixture (black lines, left axis). The specific fluorescence of PL and PL* relative to that of P are respectively 1.0 and 1.2 (A), 1.2 and 1.2 (B), 1.1 and 1.2 (C), and 1.2 and 1.1 (D).

Schemes

Scheme I.

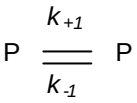

Scheme II.

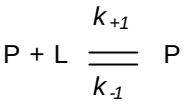

Scheme III.

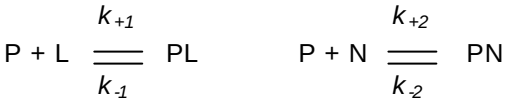

Scheme IV.

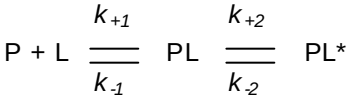

Scheme V.

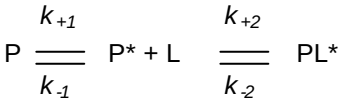

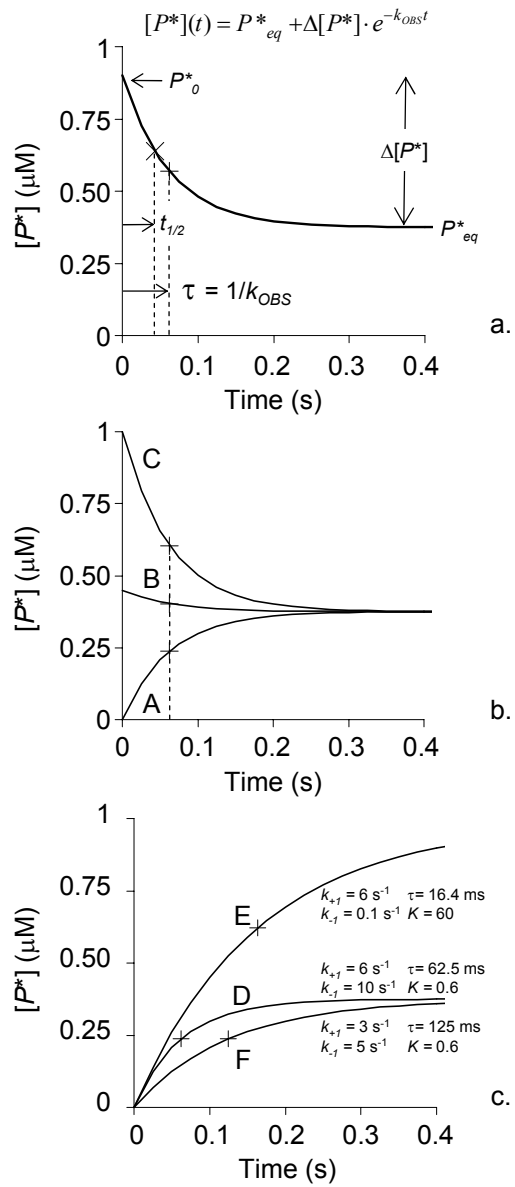

Figure 1. Transient for the reaction P ⇔ P* (Scheme **I**). Values of k_{+1} and k_{-1} were 6 and 10 s^{-1}, unless otherwise indicated; the total concentration of P, P_{tot}, was 1 μM. a) Definition of P^*_0 and P^*_{eq} (initial and equilibrium concentrations of P*), $\Delta[P^*]$ (reaction amplitude), $t_{1/2}$ (half-life), and τ (relaxation time), which is equal to the reciprocal of k_{OBS} (observed rate). b) The relaxation time is equal to $1/k_{OBS} = 1/(k_{+1} + k_{-1})$ (62.5 ms for the rate constants used here), independent of the initial concentration of P* (0, 0.45, and 1 μM in curves A, B, and C, respectively). c) If two systems have equal forward rate constants the system with the largest reverse rate constant will reach equilibrium first (curves D (k_{+1} = 6; k_{OBS} = 16) and E (k_{+1} = 6; k_{OBS} = 6.1)), whereas two systems with identical equilibrium constants may have different observed rates (curves D (K = 0.6, k_{OBS} = 16) and F (K = 0.6, k_{OBS} = 8)).

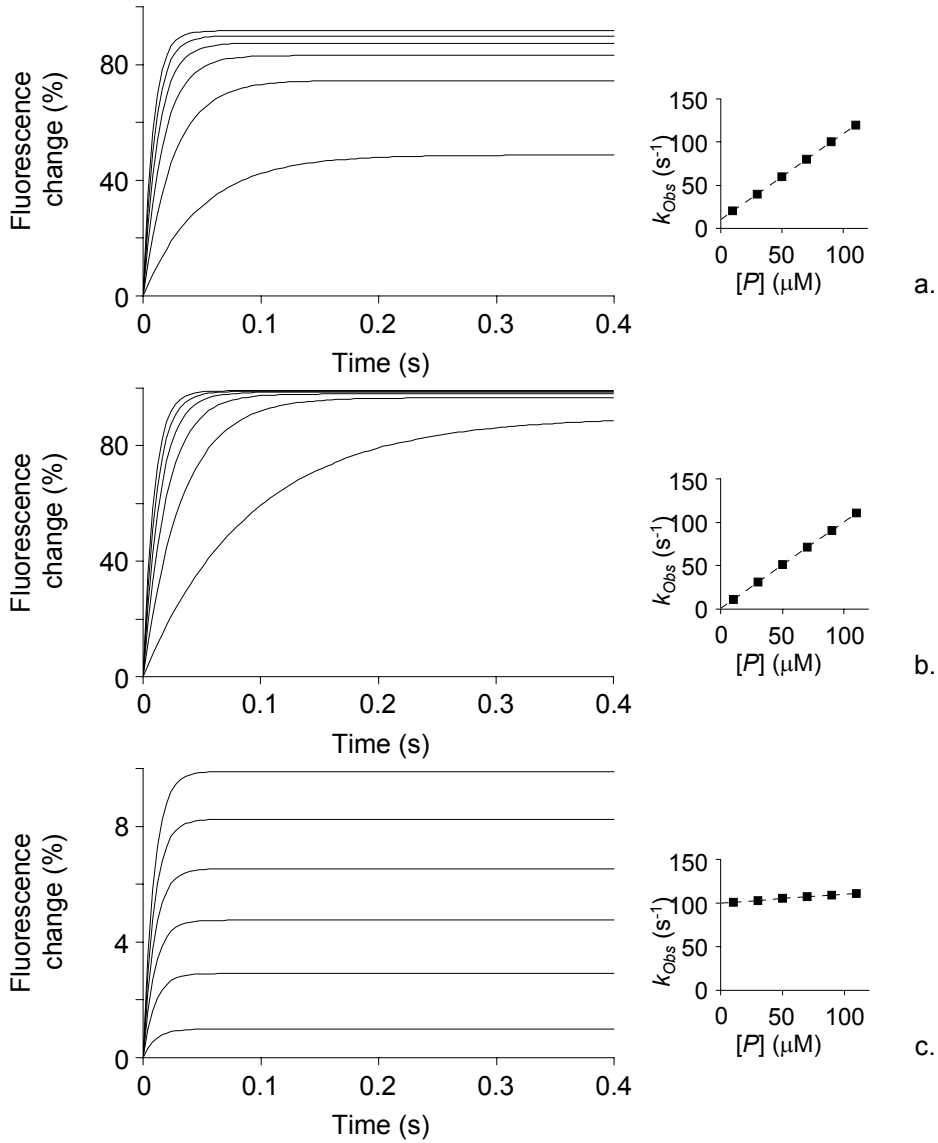

Figure 2. Left panels: typical transients (simulated) in a set of stopped-flow experiments in which a fluorescent ligand L (at 1 μM) is mixed with a large excess (10 – 110 μM) of non-fluorescent protein P. The specific fluorescence of the complex PL is higher than that of L, so that the overall fluorescence of the mixture increases as the system approaches equilibrium. The vertical axis indicates the change in fluorescence observed as a percentage of the maximal change (the difference in fluorescence between 1 μM L and 1 μM PL). Right panels: plots of the observed rates obtained from the transients versus the concentration of the component in excess (P). As $k_{OBS} = k_{+1}[P] + k_{-1}$, the slope and intercept of these plots are k_{+1} and k_{-1}, respectively. a) both slope and intercept (1 $\mu M^{-1}s^{-1}$ and 10 s^{-1}, so that K_d = 10 μM) are well-defined (have small associated errors) under the experimental conditions; b) k_{+1} is well-defined (1 $\mu M^{-1}s^{-1}$) but k_{-1} is too small (because K_d = 1 μM) to be obtained with any accuracy. c) k_{-1} is well-defined (100 s^{-1}) but k_{+1} is very small (as K_d = 1 mM in this system). Note that the affinity of P for L is so low, that at 100 μM P, only about 10% of the total L has formed PL.

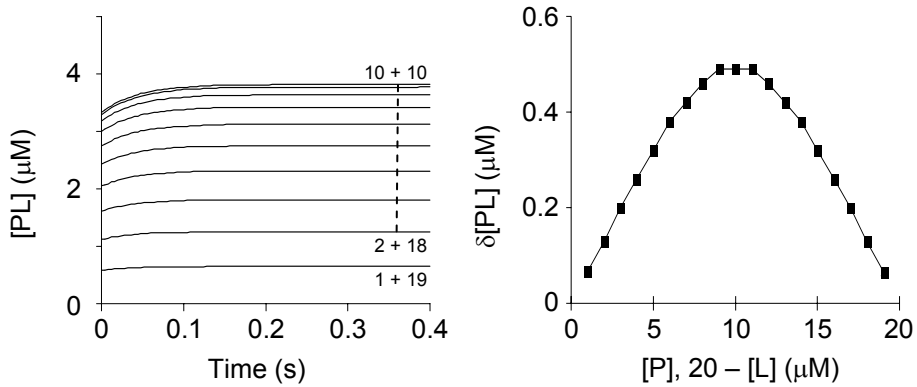

Figure 3. A set of transients (simulated) that might be observed in a temperature-jump experiment. A rapid temperature-jump (from 20 to 25 ºC) is applied to mixtures of P and L in which the sum of [*P*] and [*L*] is 20 μM, but their ratio varies. The right panel, in which the reaction amplitude Δ[*PL*] is plotted against [*P*], shows that the amplitude is maximal when [*P*]/[*L*] = 1.

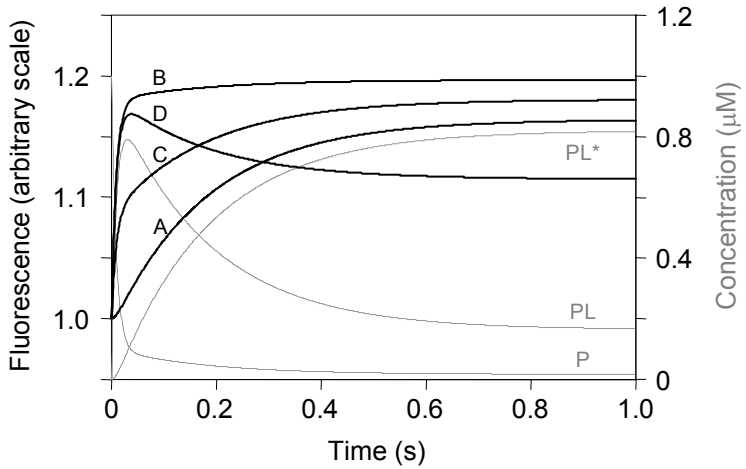

Figure 4. Relationship between the simulated time dependent changes in concentrations of P, PL, and PL* (grey lines, right axis) for the reaction scheme P + L ⇔ PL ⇔ PL* (Scheme IV, with *Ptot* = 1 μM, *Ltot* = 10 μM, k_{+1} = 10 $\mu M^{-1}s^{-1}$, and k_{-1}, k_{+2}, k_{-1} = 10, 5, and 1 s^{-1}, respectively) and the observed fluorescence of the mixture (black lines, left axis). The specific fluorescence of PL and PL* relative to that of P are respectively 1.0 and 1.2 (A), 1.2 and 1.2 (B), 1.1 and 1.2 (C), and 1.2 and 1.1 (D).